CHARACTERISTICS OF IMPATT DIODE REFLECTION AMPLIFIERS*

R.W. Laton** and G.I. Haddad
Electron Physics Laboratory, Department of Electrical and Computer Engineering
The University of Michigan
Ann Arbor, MI 48104

Abstract

The nonlinear characteristics of stable IMPATT diode reflection amplifiers including the dependence of gain, bandwidth and saturation properties upon device material, doping profile and operating conditions are given.

Introduction

Most techniques for IMPATT diode amplifier theoretical analysis rely on experimentally determined device immittance data or on Read model theory and do not address the problem of optimization of device properties for stable reflection amplifiers. The purpose of this paper is to provide an improved understanding of the design and analysis of reflection amplifiers employing the negative-resistance of IMPATT diodes, to demonstrate the validity of that theory experimentally and to examine the properties of such amplifiers and their dependence upon device material, doping profile, temperture, biasing and circuit conditions.

Nonlinear Amplifier Analysis

Previous work has shown that stable reflection gain is inversely related to the distance between points representing the admittance of a negative conductance device and the negative of its loading admittance.[1] Curves in the complex plane of such admittances as functions of frequency and RF voltage, called device-circuit (D-C) diagrams, are useful in providing rapid qualitative predictions of expected amplifier behavior and the manner in which it is affected by perturbations of device or circuit admittances. Knowledge of these admittances at a number of discrete frequencies and RF voltages might be obtained experimentally or from theoretical analyses.

Particular combinations of device and circuit which provide suitable amplifier properties, as indicated by the D-C diagram, may be analyzed in quantitative detail by means of the digital computer. Polynomial interpolation techniques are utilized to obtain admittances at closely spaced values of frequency and RF voltage, and the appropriate expression for power-wave reflection gain and voltage wave phase shift is solved at each point. Power generated by the device is uniquely determined by device conductance and RF voltage. Power input and output are related by the power wave reflection coefficient, while generated RF power is defined as the difference between input and output power at the signal frequency. Thus gain, phase-shift, input, output, and added power may be calculated at each point for which circuit and device admittance is known. One more set of interpolations may be performed to compute gain, phase-shift, and output power versus frequency for desired values of constant input power.

Experimental Verification

Fig. 1 is the D-C diagram for a p^+nn^+ Si diode in a 50 Ω coaxial circuit tuned by two quarter wave transformers with dimensions given in the upper inset. The circuit admittance was obtained by measurement, and the measured values were transformed through a lumped element equivalent circuit for the device package and mount as shown on the lower inset. The reference plane for the plotted admittances is A-A'. The kink in the circuit admittance above 9 GHz was a measured phenomena believed to be caused by the VSWR of the circulator located several wavelengths away from the tuning elements and diode. Device admittance was obtained from a large signal analysis.[2] The diode parameters were determined by measurement to be $N_d \cong 5\times10^{15}$ cm^{-3}, d ≅ 3.5 μm, area $\cong 1.0\times10^{-4}$ cm^2 where N_d and d are the doping density and length of the depletion region. Bias current density, I_o, was 950 A/cm^2 which produced a junction temperature of 260°C. Transport and ionization parameters for this temperature were linearly extrapolated from published data at 27°C and 200°C, and then an empirically determined adjustment of 10% was applied to these parameters to match the measured and predicted small signal gain peak value and frequency.

Fig. 2 shows predicted gain as a function of frequency for input power levels of -10 dBm, and 7, 16, and 23 dBm, for the conditions of Fig. 1. The pronounced dip in small signal gain at 9.25 GHz corresponds to the measured kink in the circuit admittance curve and becomes less pronounced as the separation between device and circuit admittances is increased by the higher RF voltages corresponding to larger input power.

The symbols shown near the solid curves are measured data points which demonstrate the close agreement between theory and experiment. Similar results have been obtained with GaAs diodes and circuit admittances which were calculated from the geometry of the tuning elements instead of being measured directly.

Power Added and Stable Gain

The maximum power which can be added to an input by a negative resistance device is equal to the maximum power which the same device can generate as a free running oscillator. The gain at which such maximum power addition takes place is dependent upon the device I-V relationship in the stable case and may differ for various kinds of negative-resistance devices. It may also differ for a specific device such as an IMPATT diode under different operating conditions, doping profiles, or device materials. The model described above has been utilized to study this phenomena for n-type GaAs and Si diodes, as well as the complementary Si structure. Figs. 3 and 4 show results for the "p" and "n" type Si devices at a bias current density of 500 A/cm^2 and room temperature. Three curves of gain versus RF voltage are shown for each diode, corresponding to separate choices of load providing 30, 20, and 10 dB of stable small signal gain. Results are shown for a fixed frequency selected to optimize the maximum added power. Fig. 3 indicates that at 12 GHz, 800 mw of generated power can be added by an n^+pp^+ Si X-band diode of 1.6×10^{-4} cm^2 area, and that 6 dB of gain for an output power of 1 W can be expected when the stable small signal gain is 30 dB. For 10 dB of small signal gain, maximum power is added with 3 dB of large signal gain, giving an output power of 1.6 W.

In Fig. 4 the predicted gain and power added relation is shown for the p nn Si diode with other conditions the same as the previous case. A maximum of 500 mw of power added at 3 dB of gain is predicted, independently of small signal gain. Such an amplifier would

*This work was supported by the Air Force Systems Command's Rome Air Development Center under Contract No. F30602-71-0-0099.
**Now at MIT, Lincoln Laboratory, Lexington, Mass.

provide 1 W of output power.

Results for GaAs diodes were found to be similar to those for the n^+pp^+ Si device at similar bias current densities. Finally, all the structures showed a marked deterioration in gain available at maximum power addition as the small signal gain peak was made to approach the avalanche frequency because of the increasing dependence of device susceptance on RF voltage. This manifests itself in the frequently observed phenomena of gain expansion with increasing input power at frequencies below the small signal gain peak, and is most prominent at frequencies near the avalanche frequency.

Fig. 5 indicates experimental results showing the dependence of gain saturation and frequency response on bias current density when the circuit tuning is changed to provide approximately equal values of small signal gain and frequency. In the first case, 21 dB of small-signal gain at 9.4 GHz was obtained with a bias current density of 500 A/cm^2. Tuning was accomplished with two coaxial slugs, and gain was measured at input power levels of -20, 0, 10 and 16 dBm. Bias current density was then increased to 1000 A/cm^2, a new tuning condition obtained which produced 19 dB of small-signal gain at 9.2 GHz, and measurements taken for the same input power levels.

Several differences in amplifier properties are evident. At the lower current density the gain compression between small-signal drive and an input power level of 40 mw was 16 dB, while the shift in f_p was approximately 125 MHz toward the lower frequency end. At the higher current density the gain compressed by 11.5 dB between small-signal and 40 mw input power levels. Thus the output power at this drive level was approximately 5 dB higher for the 1000 A/cm^2 bias condition and the RF conversion efficienty was approximately 2.7% versus 1.5% for the 500 A/cm^2 case. Next, because the avalanche frequency increased with bias current density, f_p was closer to the avalanche frequency at the higher current density, and the shift downward in frequency with increasing drive levels was more pronounced. The instantaneous bandwidth and gain-bandwidth product were larger for the higher current density case at all levels of input power.

Broadbanding Capability of IMPATT Devices

Differences in the small-signal device quality factor Q_d, defined as B_d/G_d, may be seen from the admittance characteristics of the various devices studied previously, which suggests that there are differences in the instantaneous fractional bandwidth of amplifiers employing these different devices. The optimum fractional bandwidth obtainable from each device has been determined according to methods based on Bode-Fano matching techniques.[3] These are strictly applicable only when the device can be modeled by a frequency-independent shunt -G and C. For amplifiers with large small-signal gain, i.e., 30 dB, optimum fractional bandwidths are of the order of 5% and the departure from constant device conductance and linear frequency dependence of device susceptance is not too great. The realization of the ultimate bandwidth at lower gain levels dictates the synthesis of a circuit by means of a more complex lossy model for the device, such as proposed by Ku and Scherer.[4]

This analysis indicates that the double-drift structure provides the maximum broadbanding capability followed by the ideal Read, p-type and n-type structures in that order for unpackaged devices, and that the package impedance transformation in the coaxial circuit reduces instantaneous bandwidth which can be obtained by 20 to 30% for each structure.

Broadbanding capability has also been investigated at several different bias current densities and at elevated temperatures which correspond more closely to actual operating conditions for normally encountered values of thermal resistance and forced air or water cooling. In order to permit device comparison vs. frequency, a $1/Q_A$ factor is used as a figure of merit in this section. Curves of $1/Q_A$ as a function of frequency provide a direct comparison of instantaneous fractional bandwidth for a fixed gain and ripple. Fig. 6 shows the factor $1/Q_A$ vs. frequency for the n-type Si diode at 500 and 1000 A/cm^2 at room temperature, 500 A/cm^2 at 100°C and 1000 A/cm^2 at 200°C. The device structure is the same as that studied in the previous section except for the elevated temperatures in which the n-region width has been reduced to 3.5 μm to retain a negative conductance peak near 12 GHz. It is shown in Fig. 6 that the broadbanding capability is improved by increased values of bias current, although the improvement is not as great when the rise in temperature which accompanies higher current levels is considered. Similar behavior is observed for the p-type Si and n-type GaAs diodes.

Conclusions

Programs have been developed which utilize the digital computer to calculate gain, phase shift and output power as functions of frequency and input power as well as the variation of gain and power added with RF voltage. These programs require knowledge of device and circuit admittances at several discrete RF voltages and frequencies.

Experimental measurements of gain as a function of frequency and input power level have been carried out utilizing Si and GaAs diodes, and excellent agreement has been demonstrated between theory and measurement.

The theoretical concepts have been utilized to study the dependence of amplifier response on doping profile, bias current density, and temperature. It has been shown that the Si n^+pp^+ device is theoretically capable of providing output powers in excess of 1.5 W at a gain of 3 dB in a stable amplifier circuit near the optimum frequency. Additional experimental results have been presented which demonstrate dependence of gain and bandwidth on bias current density and circuit tuning conditions. Gain bandwidth and power added are both enhanced by higher current densities, although both are degraded by the higher junction temperatures which accompany the higher current levels. The double-drift region Si diode offers the largest gain-bandwidth product of the structures investigated.

References

1. R.W. Laton and G.I. Haddad, "Effects of Doping Profile on Reflection-type IMPATT Diode Amplifiers," Proc. 1971 European Microwave Conf., Stockholm, Sweden, pp. A5/1:1 - A5/1:4, August 1971.

2. W.E. Schroeder and G.I. Haddad, "Nonlinear properties of IMPATT devices," Proc. IEEE, pp. 153-182, February 1973.

3. W.J. Getsinger, "Prototypes for use in broadbanding reflection amplifiers," IEEE Trans. Microwave Theory and Tech., Vol. MTT-11, pp. 486-497, November 1963.

4. W.H. Ku and E.F. Scherer, "Gain-bandwidth optimization of avalanche-diode amplifiers," IEEE Trans. Microwave Theory and Tech., Vol. MTT-18, pp. 932-942, November 1970.

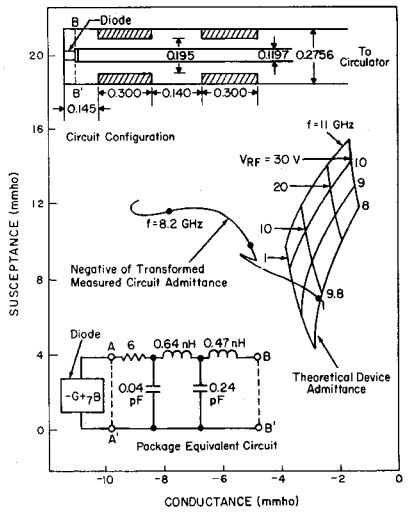

FIG. 1 DEVICE-CIRCUIT DIAGRAM OF EXPERIMENTAL Si-DIODE AMPLIFIER

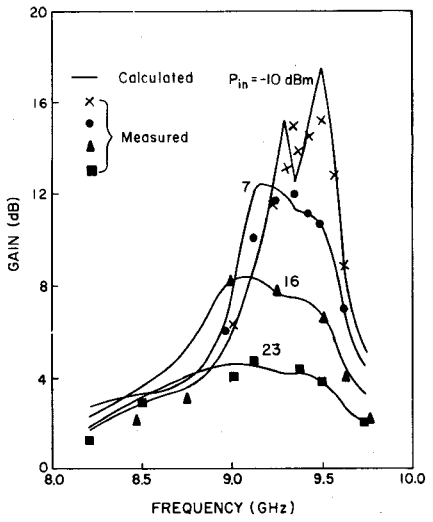

FIG. 2 PREDICTED AND MEASURED RESPONSE VS. INPUT POWER

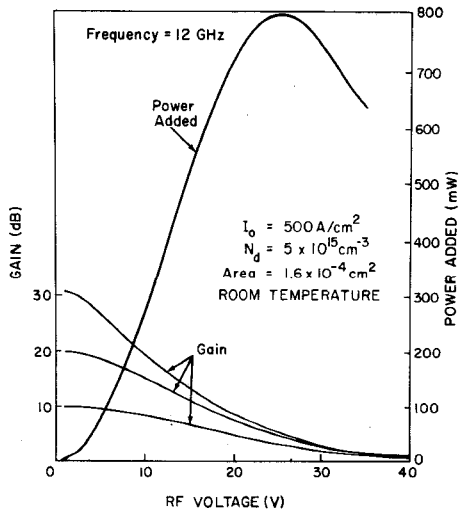

FIG. 3 POWER AND GAIN AT 12 GHz (Si n^+pp^+ DIODE)

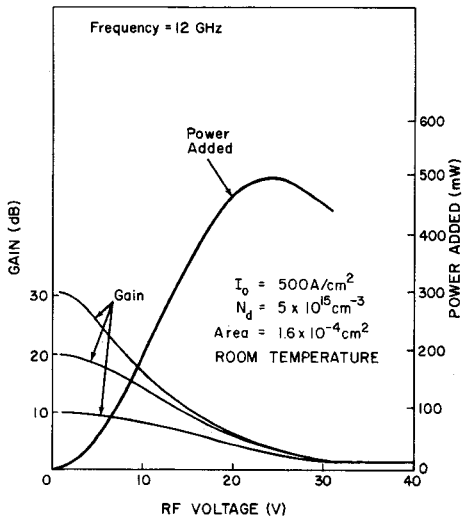

FIG. 4 POWER ADDED AND GAIN AT 12 GHz (Si p^+nn^+ DIODE)

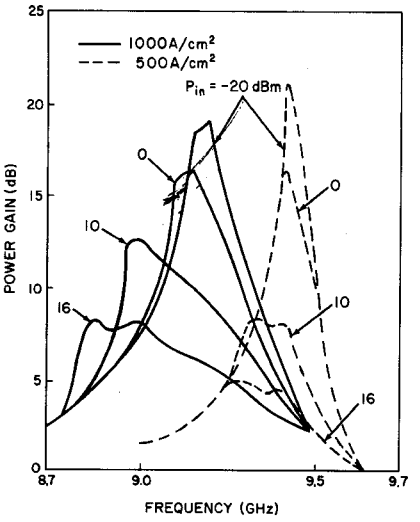

FIG. 5 MEASURED RESPONSE AT SEVERAL BIAS CURRENT DENSITIES

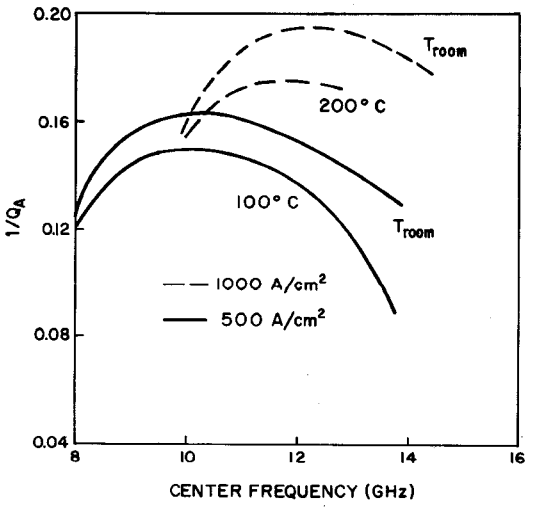

FIG. 6 BROADBAND CAPABILITY DEPENDENCE ON TEMPERATURE AND BIAS (Si p^+nn^+ DIODE)